

Study of the Trends of Chemical–Physical Parameters in Different Karst Aquifers: Some Examples from Italian Alps

*Original*

Study of the Trends of Chemical–Physical Parameters in Different Karst Aquifers: Some Examples from Italian Alps / Balestra, Valentina; Fiorucci, Adriano; Vigna, Bartolomeo. - In: WATER. - ISSN 2073-4441. - ELETTRONICO. - 14:3(2022), p. 441. [10.3390/w14030441]

*Availability:*

This version is available at: 11583/2954380 since: 2022-06-21T17:18:53Z

*Publisher:*

MDPI

*Published*

DOI:10.3390/w14030441

*Terms of use:*

This article is made available under terms and conditions as specified in the corresponding bibliographic description in the repository

*Publisher copyright*

(Article begins on next page)

## Article

# Study of the Trends of Chemical–Physical Parameters in Different Karst Aquifers: Some Examples from Italian Alps

Valentina Balestra \*, Adriano Fiorucci and Bartolomeo Vigna

Department of Environment, Land and Infrastructure Engineering (DIATI), Politecnico di Torino, Corso Duca degli Abruzzi 24, 10129 Torino, Italy; adriano.fiorucci@polito.it (A.F.); bartolomeo.vigna@polito.it (B.V.)

\* Correspondence: valentina.balestra@polito.it; Tel.: +39-011-0907714

**Abstract:** The results of a series of continuous characterizations of physical parameters (flow, temperature, water conductivity) and chemical analyses in water springs fed by karst aquifers located in the Piedmont region (northwestern Italy) are presented in this work. Rock masses in carbonate rocks, characterized by very different hydrogeological situations, linked to a different degree of karstification, fracturing, and development of the saturated zone, were examined. A series of data-loggers were installed, operating for several years, and different water sampling missions and subsequent chemical analyses (main ions, metals, and rare earth elements) under different hydrodynamic conditions were carried out. The results show very different trends of chemical–physical water parameters, particularly following significant infiltrative events. Aquifers characterized by a high karstification and reduced saturated zone highlight water mineralization decreases, even within a few hours, as a result of significant flow rate increases (prevalent substitution). Aquifers with a well-developed saturated zone, during an entire flood event, highlight an increase in mineralization linked to the remobilization of water present in the less permeable sectors of the aquifer (piston flow phenomenon). Lastly, aquifers fed by very fractured rocky masses and reduced karstification have a water flow rate with mild annual variations and constant chemical–physical parameters over time (homogenization phenomenon).

**Keywords:** aquifers in carbonate rocks; karst; springs; monitoring; water geochemistry



**Citation:** Balestra, V.; Fiorucci, A.; Vigna, B. Study of the Trends of Chemical–Physical Parameters in Different Karst Aquifers: Some Examples from Italian Alps. *Water* **2022**, *14*, 441. <https://doi.org/10.3390/w14030441>

Academic Editors: Slobodan Miko and Nikolina Ilijanić

Received: 16 December 2021

Accepted: 28 January 2022

Published: 1 February 2022

**Publisher's Note:** MDPI stays neutral with regard to jurisdictional claims in published maps and institutional affiliations.



**Copyright:** © 2022 by the authors. Licensee MDPI, Basel, Switzerland. This article is an open access article distributed under the terms and conditions of the Creative Commons Attribution (CC BY) license (<https://creativecommons.org/licenses/by/4.0/>).

## 1. Introduction

Karst aquifers occur in many areas of Europe, from the alpine mountain sectors (high-altitude Pyrenees, French, Swiss, Austrian, Italian karst) to the Apennines and the medium- and low-altitude areas of the karst overlooking the Mediterranean [1–9]. The hydrodynamic regime of these aquifers is affected by the local meteorological conditions [2–5], the geological and structural order, the karstification degree, and the rock cluster fracturing. The hydrogeology of these massifs was discussed in different works (e.g., [1,7–24]). The velocity of the water flow in the drainage network, the presence/absence of large saturated zones (and, therefore, the water time of permanence in the drainage network), and the rock–water contact evidently affect the main spring water chemical–physical parameters [14,25–27].

The spring hydrodynamics is influenced by the hydraulic pressures in the discontinuity network of karstic channels, and some chemical–physical water parameters, such as temperature and electric conductivity, can highlight this important phenomenon [21,25,28–34]. Taking into account the drainage system, three different basic conceptual aquifer models can be distinguished: systems with dominant drainage (high permeability, absent or reduced phreatic zone), systems with interconnected drainage (high permeability, extensive phreatic zone), and systems with dispersive circulation (middle–low permeability, very extensive phreatic zone) [14,21,26,34–39]. Various intermediate situations exist; however, on the basis of spring hydrography and hydro-chemical monitoring, it is always possible to refer to one of these models for describing a karst system [30].

The aquifers are characterized by systems with dominant drainage feed springs located in correspondence to a limit of permeability, between less permeable rock and the aquifer above. Sometimes, these springs can also be located at a higher altitude than the local base level (perched springs). These systems have a high degree of karstification and an absent or reduced phreatic zone. A well-organized outflow network with a series of main natural tunnels and secondary drains characterizes these kinds of aquifers. The neo-infiltrating waters move rapidly in the discharge area, mixing slightly with the resident waters. The response to rainfall is very fast (few hours), and the outflow velocities can exceed 400 m/h in flood conditions, with marked flow variations depending on the local meteorological regime [14]. The geochemistry of the spring water with dominant drainage suffers from the presence of preferential drainage pathways and of a reduced phreatic zone. A sudden decrease in the mineralization values can be observed during important infiltration events. The neo-filtration water, still aggressive and slightly mineralized, reaches the emergence zones quickly, replacing the water circulating in the system (prevalent substitution). Therefore, an increase in the flow and a decrease in the temperature occur, even after a prolonged period of drought.

In systems with interconnected drainage, springs are located close to the permeability threshold, characterized by a subvertical contact between the impermeable rocks and the aquifer. Generally, at the same altitude, a relatively developed saturated zone is present. The phreatic conduits are generally present in moderately karstified fractured rock massifs. The spring flows undergo a significant increase during rainfall events. Near the saturated zone, the fresh water causes an important water level rise, with a consequent transmission of hydraulic pressure in the fracture network and in the phreatic conduits (piston flow phenomenon). Consequently, an almost instantaneous water level increase, related to the remobilization of resident waters and characterized by a high mineralization, is generated. Therefore, the piston flow phenomenon can be highlighted by some chemical–physical groundwater parameters, such as temperature and electric conductivity [21,25,28–30,32–34]. During snowmelt, the first part of the flood begins, and the piston flow phenomenon can clearly be seen, highlighted by an increase in water level, temperature, and electric conductivity values.

Lastly, the systems with dispersive circulation feed springs located next to the lower sectors of the aquifer structure, which are often situated close to the valley bottom. These systems are typical of extremely fractured carbonate rock masses and are not characterized by any preferential water pathways. They have a very reduced or even inexistent karstification, and the saturated zone is very extensive. Permeability is normally low, due to the small dimensions of the fracture systems, and the flow velocities are rather low. The discharge increases are not connected to the individual infiltration recharge and occur some days after the beginning of the input event. The physical–chemical parameters of groundwater in systems with dispersive circulation are constant over time, and they have modest seasonal variations. The neo-infiltration water descends over a very long period, losing the external signal and reaching a remarkable equilibrium with the rocks (homogenization phenomenon); therefore, the water mineralization level is usually rather high.

Knowledge of karst system hydrogeology, its vulnerability, and karst spring behavior is interesting because these aquifers represent an important source of potable water [37,40–43]. Although the conceptual models of groundwater circulation in carbonate mass rock and the chemical–physical aquifer response have been described, only a few studies provided concrete examples of how to feed a karst system (e.g., [14,38,44–46]). The aim of this study was to describe six carbonate aquifers of the southern Alpine chain of Piedmont, northwestern Italy, showing the evident hydrodynamic differences between the types of groundwater circulation in a carbonate cluster and the hydro-chemical response of these aquifers to infiltrative input. A high-frequency monitoring of the main parameters (flow rate, electrical conductivity, and water temperature) was conducted, together with chemical analyses on a series of collected water samples.

## 2. Materials and Methods

### 2.1. Study Area

Extensive outcrops of carbonate rocks belonging to the Brianzonesi, Sub-Brianzonesi, and Pre-Piemontesi units characterize the study area (southwestern Piedmont, Italy) (Figure 1, Table 1).

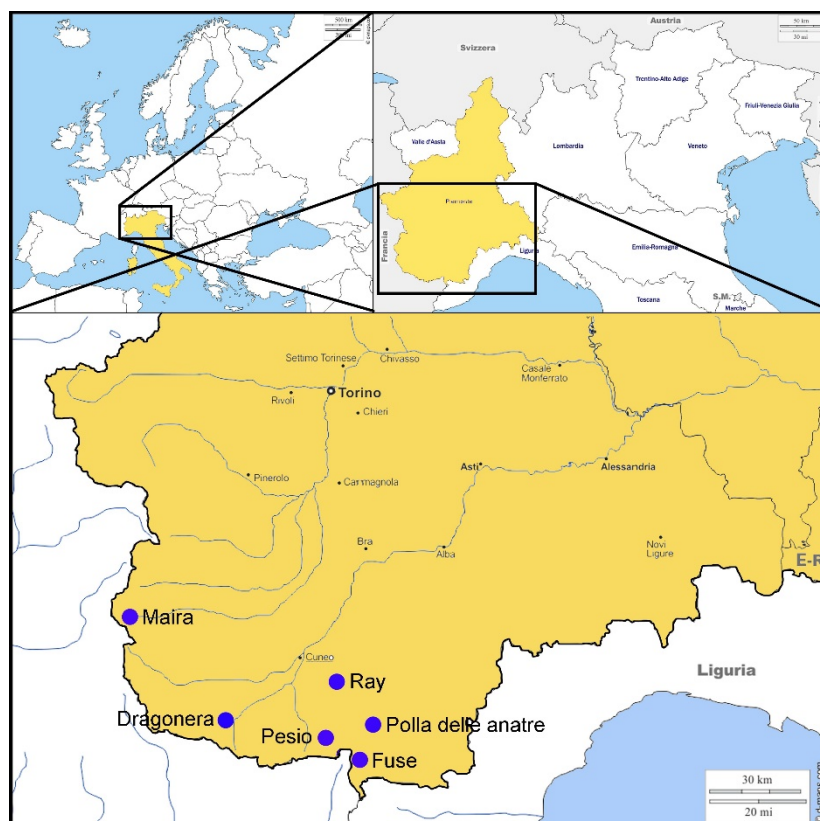


**Figure 1.** Location of the monitored springs (southwestern Piedmont, Italy). Maps used for the plate were modifications of those retrieved from [https://d-maps.com/carte.php?num\\_car=2232&lang=en](https://d-maps.com/carte.php?num_car=2232&lang=en) (accessed on 11 March 2021), [https://d-maps.com/carte.php?num\\_car=5894&lang=en](https://d-maps.com/carte.php?num_car=5894&lang=en) (accessed on 11 March 2021), and [https://d-maps.com/carte.php?num\\_car=8273&lang=en](https://d-maps.com/carte.php?num_car=8273&lang=en) (accessed on 11 March 2021)).

**Table 1.** Basic characteristics of the monitored areas and of the six examined spring.

Spring	Tectonic Units	System	Chemical Signal	Saturated Zone	Karstification
Pesio	Brianzonesi units	Dominant drainage	Prevalent substitution	Absent or reduced	High
Fuse	Brianzonesi units	Dominant drainage	Prevalent substitution	Absent or reduced	High
Dragonera	Sub-Brianzonesi units	Interconnected drainage	Piston flow phenomenon	Extensive	Moderate
Polla delle anatre	Brianzonesi units	Interconnected drainage	Piston flow phenomenon	Extensive	Moderate
Maira	Brianzonesi units	Dispersive circulation	Homogenization phenomenon	Extensive	Reduced or inexistent
Ray	Pre-Piemontesi units	Dispersive circulation	Homogenization phenomenon	Extensive	Reduced or inexistent



In the outermost areas of the Alpine chain, the karst massifs have minor deformations, and the carbonate rocks are slightly fractured and detached from the impermeable rocks of the metamorphic basement, which is often located at a high altitude. For this reason, springs are also located at hundreds of meters above the valleys (e.g., Pesio and Fuse springs) (Table 1). Above 2000 m, vast calcareous plateaus are present (Marguareis and Mongioie massifs). The calcareous–dolomitic succession of this area shows bare karst surfaces, generally characterized by compact rocks outcrop with numerous karren [14]. This surface morphology facilitates a very rapid infiltration of the rainwater and the snowmelt water [14]. A very extensive karst system is present in this area; karst complexes can develop even for several dozens of kilometers, with more than 1000 m of altitude difference. Some of these cavities reach the metamorphic basement rocks, and some active tunnels flow in the metavulcanites. The saturated zone of these systems is almost absent; therefore, well-developed karst conduits (phreatic conduits) are present, and they are able to drain important water volumes after abundant recharge events [30]. The recharge area of Pesio spring (Figures 1 and 2A) (18 km<sup>2</sup>), located in Marguareis Park, is between 2400 and 1380 m a.s.l. [30], and the current water circulation level is at about 160 m under a network of large and dry tunnels with a phreatic morphology. The Pesio spring is also an important attraction for tourism during spring season, when a spectacular waterfall (Pis del Pesio) flows out of a karst conduit above the spring. The Fuse spring (Figures 1 and 2B) is located in the upper Tanaro valley, a few hundred meters from the Vene spring, at an altitude of 1460 m a.s.l. The feeding area of these two springs (12 km<sup>2</sup>) is located in the karst massif of M. Mongioie (2630 m a.s.l.), in the upper Ellero valley. This area is characterized by the presence of a spectacular bare karst with extensive furrowed fields areas.

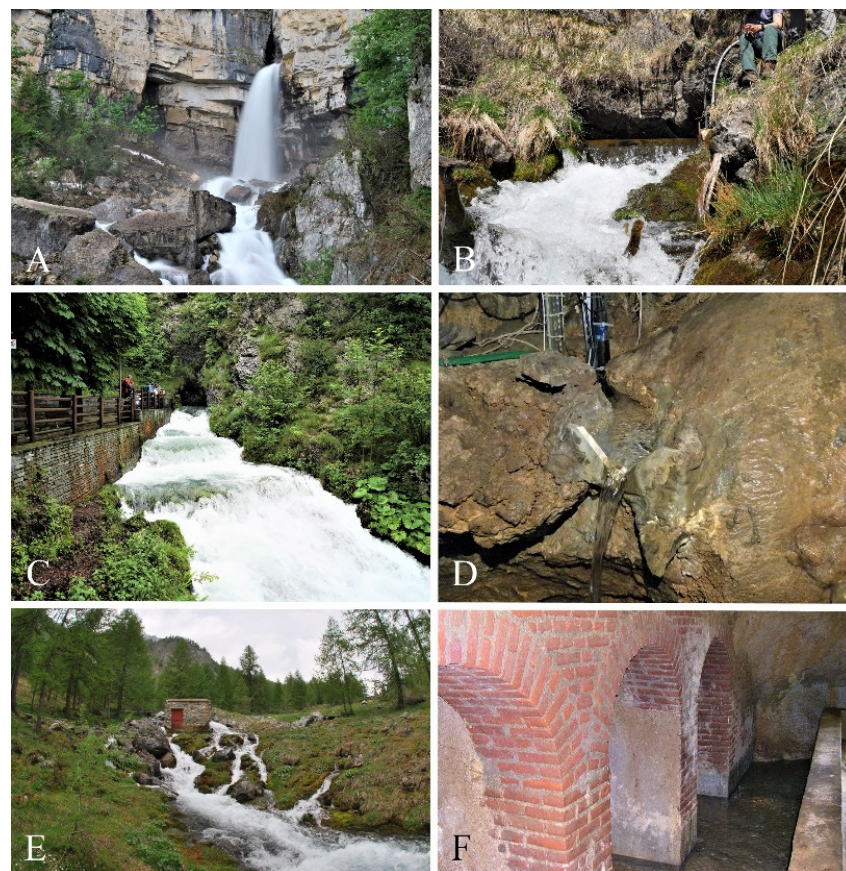


**Figure 2.** Examined karst springs in Piedmont Region, NW Italy. (A) Pesio spring; (B) Fuse spring; (C) Dragonera spring; (D) Polla delle anatre spring; (E) Maira spring; (F) Ray spring. Photos by Bartolomeo Vigna.

In the innermost areas of the Alpine chain, the karst massif has major deformations. Systems, which supply springs with much more regular flows, are present in the areas with more fractured rock masses. Therefore, the soil is more abundant, and only few or no superficial and deep karst morphologies are present. The carbonate rock mass is delimited by impermeable metamorphic bedrock, which generally produces an extensive saturated zone (e.g., Dragonera and Polla delle anatre springs) (Table 1). The Dragonera spring (Figures 1 and 2C) is supplied by a karstic fractured aquifer with a medium–high permeability, and it is characterized by a low level of karstification and wide saturated zone [30]. The recharge area of this spring (8.5 km<sup>2</sup>) is between 1950 and 840 m a.s.l., and the recharge is mainly of the diffuse type, but there is also a contribution from small adjacent porous aquifers. The Polla delle anatre spring (Figures 1 and 2D) is a secondary coming flowing into the Bossea cave karst river. Its recharge area extends on Corsaglia valley, between 900 and 1000 m a.s.l., and it has an extension of less than 1 km<sup>2</sup>. This area is characterized by intensely fractured marble limestone.

In the inner zones of the Alpine chain with intensive deformations, dolomites and dolomitic limestones have been fractured. In these massifs, deep karstification is limited, and the saturated zone is very extensive. Springs are always located in the lower zone of the carbonate rocks, in correspondence with the permeability threshold and the metamorphic base (e.g., Maira and Ray springs) (Table 1). The Maira spring (Figures 1 and 2E) has a considerable importance for its average flow rate, reaching one of the highest values of the whole Piedmont region (700 L/s). Moreover, it is used for electricity production. The recharge area is located at the ridge separating the Maira Valley (Italy), the Orrenaye Valley (France), and smaller valleys in the Ubaye Valley (France). This area is located mainly over 2500 m a.s.l., and it is characterized by dolomitic limestone and dolomite. Despite the presence of numerous endorheic basins, which facilitate the infiltration of surface waters, deep karstification is very limited. At the base of the carbonate succession, an evaporitic complex consisting of gypsum and anhydrite is present, constituting very limited outcrops. The basal complex, consisting mainly of quartzites and metavulcanites, is an important permeability threshold that conditions the underground flow to the spring area. The Maira spring water emerges through a series of little springs located at the bottom of the rock wall of M. Arpet (1650 m a.s.l.). The recharge area of Ray spring (2.5 km<sup>2</sup>) (Figures 1 and 2F), between 780 and 620 m a.s.l., is characterized by a thick blanket of residual deposits of clay and silt over the karst and by the presence of vast endorheic basins [30]. The dolomite aquifer that feeds Ray spring is intensely fractured with a very slowly flowing water, typical of a dispersive circulation system. The flow rate remains relatively constant over time.

The six examined carbonate aquifers are situated in the mountain area of the Mediterranean basin, in a pluvial-snow-type meteorological regime [14,47,48]. All springs are located in areas influenced by an alpine climate, featuring the main rainfall events in spring and autumn and the snow in winter [14].

The snowfall processes mainly influence the trend of the yearly aquifer flow. From November to April, a period characterized by low temperatures, snowfall accumulates on the ground. With the progressive increase in the air temperature during the spring season, the melting process starts. The flow of the dominant drainage systems rises with a series of marked daily oscillations, reaching the minimum values in the morning and the maximum value in the evening [14]. The flooding gradually diminishes in the summer months. Moderate daily variations due to the important flooding related to snowmelt and spring rainfall also characterize the interconnected drainage systems. In this case, the daily peaks are related to the transmission of the hydraulic pressure, which acts in the water present in the network system of the saturated zone [14]. In the dispersive circulation systems, the spring flood persists for a long time. The discharge decreases slowly in the dense network of rock microfractures; therefore, the flow is relatively abundant during the winter period, being conditioned by the autumn rainfall from the previous year. The discharge at the spring rises very slowly because of the rain or snowmelt, until it reaches a maximum yearly value at the end of the springtime. It follows a depletion curve until

autumn [14]. The heavy autumn rainfall in the high-altitude recharge areas also contributes to feeding the aquifers.

## 2.2. Methodology

Data used in this study have been collected since 2006 by Politecnico di Torino and Regione Piemonte on different springs. To describe the three conceptual models, the results of the six most significant springs were considered to describe the three conceptual models: Maira, Pesio, Polla delle anatre, Rai, Dragonera, and Fuse springs. Other examined springs show hydrogeological and geochemical intermediate situations compared to those considered.

Different automatic detectors were installed to continuously monitor water quantitative and qualitative data such as flow rate (Q), temperature (T), and electric conductivity (EC). The flow rate was calculated through overflow vents or calibrated flow sections, giving the water levels. A real-time OTT monitoring system was used for hydrogeological parameter measurements (double-graphite-cell EC sensors: accuracy 0.5% mv, T probes: resolution 0.1 °C, accuracy 0.5 °C, ceramic capacitive water level measurement cells: resolution 1 mm, accuracy 0.05% fs). Hourly data acquisitions were done.

The most significant periods of each spring were taken into account to highlight the hydrogeological and geochemical situations of the three conceptual models. For an overview, annual data were considered for each spring (Figure 3). Moreover, to show different characteristic events of systems with dominant and interconnected drainage, daily data were taken into account (Figure 4).

Several spring water samples were taken during the surveys, under different hydrodynamic conditions (from dry periods to high flow rates). Chemical analyses were carried out on these samples at the Laboratory of Applied Hydrogeology of Politecnico di Torino to determine the major ion content ( $\text{Ca}^{2+}$ ,  $\text{Mg}^{2+}$ ,  $\text{Na}^+$ ,  $\text{K}^+$ ,  $\text{Cl}^-$ ,  $\text{SO}_4^{2-}$ ,  $\text{HCO}_3^-$ , and  $\text{NO}_3^-$ ) (Supplementary Tables S1 and S2). Calcium and magnesium were determined by ion-selective complexometric titration and automatic potential control. Sodium and potassium were determined by flame atomic absorption spectrometry. Chlorides, sulfates, and nitrates were determined by liquid-phase ion chromatography, while bicarbonates were determined by acid–base titration with  $\text{H}_2\text{SO}_4$  0.5 N and automated continuous pH measurement.

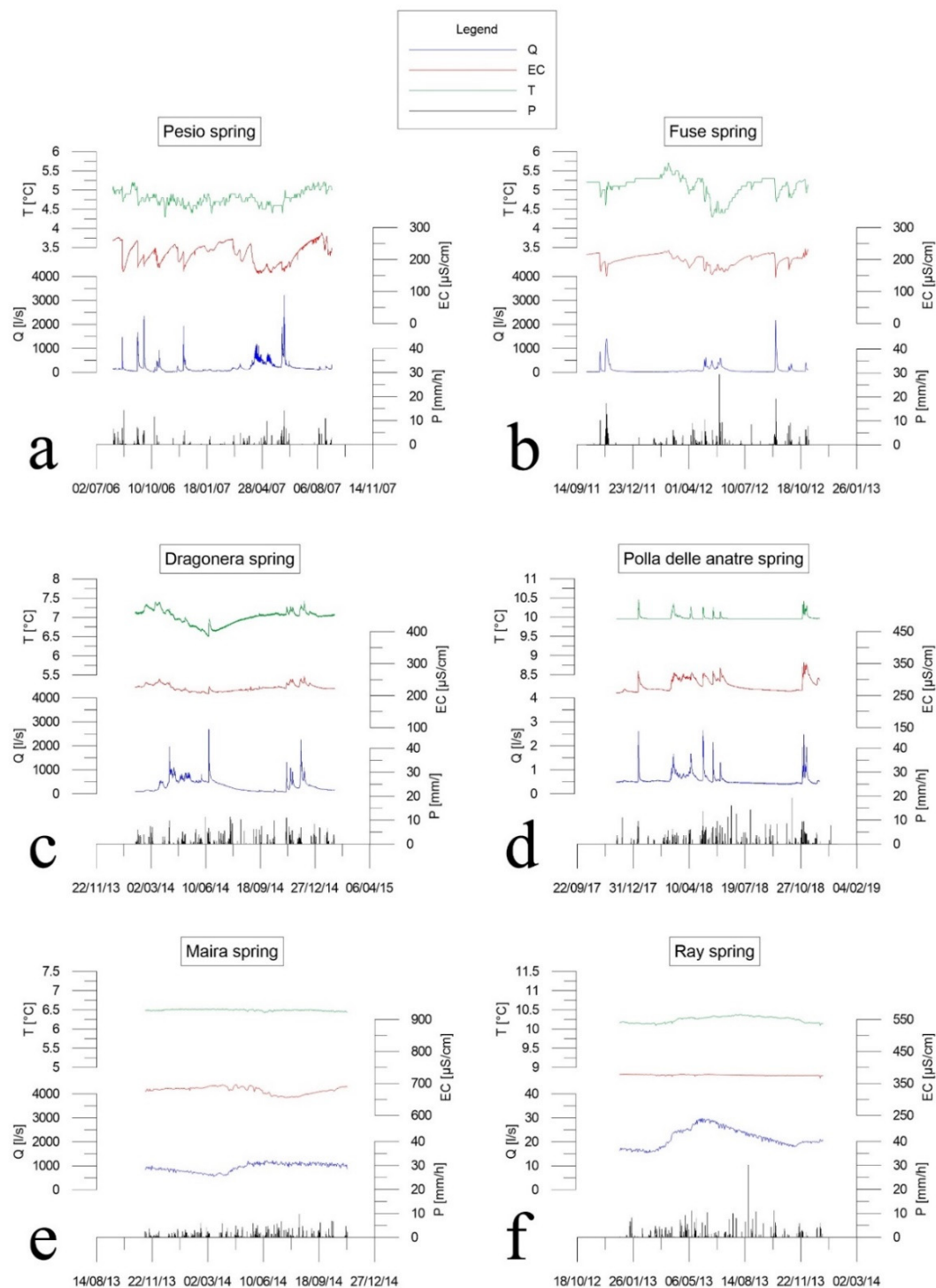


**Figure 3.** Annual water flow rate (Q), temperature (T), and electric conductivity (EC) of the six examined springs and annual precipitation (P) in the examined spring areas. Data on precipitation in areas surrounding springs were retrieved from <http://www.arpa.piemonte.it/> (accessed on 15 January 2022). (a) Pesio spring, system with dominant drainage; (b) Fuse spring, system with dominant drainage; (c) Dragonera spring, system with interconnected drainage; (d) Polla delle anatre spring, system with interconnected drainage; (e) Maira spring, system with dispersive circulation; (f) Ray spring, system with dispersive circulation.



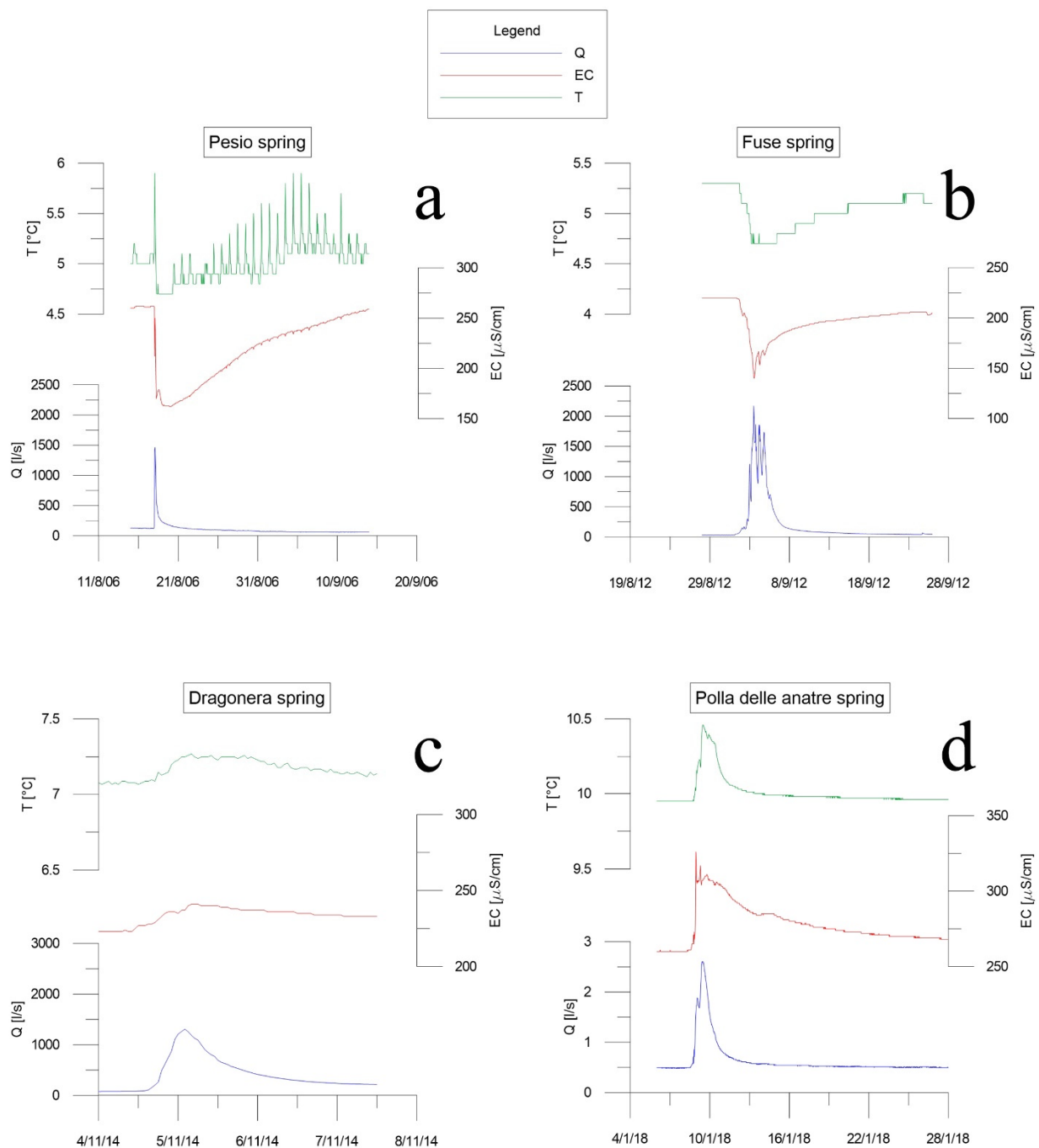


**Figure 4.** Water flow rate (Q), temperature (T), and electric conductivity (EC) of the six examined springs during a seasonal event. (a) Pesio spring, system with dominant drainage; (b) Fuse spring, system with dominant drainage; (c) Dragonera spring, system with interconnected drainage; (d) Polla delle anatre spring, system with interconnected drainage.

### 3. Results and Discussion

#### 3.1. Systems with Dominant Drainage and Prevalent Substitution

The Fuse and Pesio springs are fed by karst aquifers highly karstified. These springs have an extremely variable hydrodynamic regime (Figure 3a,b), characterized by a significant and rapid increase in Q, following the main infiltration events (rain and snow melting), and by very low Q values without direct inputs. The examined monitoring period was carried out in 2006–2007 for Pesio spring and in 2011–2012 for Fuse spring (Figure 3a,b).

In the winter season, the water flow is weak and constant, due to low air temperatures that slow down the infiltration processes. The water flow in Fuse and Pesio springs  $Q$  was about 30 and 40 L/s, respectively. The water EC and  $T$  values remained rather constant or rose slightly, due to very low water flows, in contact with the rocks. The Fuse spring EC was around 220  $\mu\text{S}/\text{cm}$ , while it was about 260  $\mu\text{S}/\text{cm}$  for Pesio spring.

With the air temperature increasing, usually from March to June, a very important period of flooding begins, linked to the snow melt processes. This flood is characterized by marked daily water flow variations, linked to the increase in air temperatures in the afternoon, reaching 700–800 L/s. The peak values of the Fuse and Pesio springs were relatively low and did not exceed 1000 L/s because they were linked to a winter season, characterized by low snowfall. Further increases in the flow rate occur in the spring season, due to the abundant rains, reaching the maximum peaks values. The chemical–physical parameters of the water clearly underline the beginning of the spring flood, highlighting temporary flow rate increments, and  $T$  and EC decrements (Figure 3a,b). The decrease in  $T$  and EC values is connected with the hydrodynamic regime, related to the neo-infiltrating water mixing, much colder and less mineralized than circulating water in the rock massif. During this period, the  $T$  of Fuse and Pesio springs reached 4.2 °C and 3.8 °C, respectively, the minimum annual values. The EC of Fuse and Pesio springs decreased from 220 to 140  $\mu\text{S}/\text{cm}$  and from 260 to 155  $\mu\text{S}/\text{cm}$ , respectively.

Starting from June, the flow rates decrease, and the water chemical–physical parameters increase progressively until they stabilize, reaching values similar to those measured in the winter season. The late summer precipitations, particularly in October and November, cause marked  $Q$  peaks, generally reaching the maximum annual values. Within a few hours, the flow rate increased from a few tens of L/s to over 2500 L/s for the Pesio spring (Figure 3a) and over 2000 L/s for the Fuse spring (Figure 3b). Within a few days, the water flow returned to the previous infiltrative event values. Water  $T$  and EC values temporarily decreased, due to the colder and less mineralized neo-infiltration water. The EC values of Pesio and Fuse springs decreased of about 70–100  $\mu\text{S}/\text{cm}$  within a few hours, reaching the annual minimum values, quite similar to the spring flood ones.

To highlight the prevalent substitution response of these two springs, two examples are reported in Figure 4a,b. On 17 August 2006, the Pesio spring  $Q$  even increased from 120 to 1466 L/s in about 4 h, while EC and  $T$  values decreased from 262 to 170  $\mu\text{S}/\text{cm}$  and from 5.0 to 4.7 °C in 8 h (Figure 4a). On 25 October 2011, the Fuse spring  $Q$  rose from 24 to 1490 L/s in only 14 h, while the water EC and  $T$  values decreased from 220 to 154  $\mu\text{S}/\text{cm}$  and from 5.3 to 4.8 °C in about 19 h (Figure 4b).

At the end of the autumn, the air temperature influences the hydrodynamic and chemical–physical parameters of the water. In cold years, snowy precipitations also characterize low altitudes with very reduced infiltration processes. As a result of rains occurring in these periods, especially due to the climate change, few marked floods are observed, equally evidenced by a decrease in water  $T$  and EC values (piston flow phenomenon).

Chemical data from Pesio and Fuse spring samples show a clear difference between maximum and minimum water flow periods (Supplementary Tables S1 and S2). In the Pesio spring (Figure 5a), water chemism passed from primary bicarbonate–calcic facies with sulfate–magnesian sub-facies in the lean period to a bicarbonate–calcic–magnesian facies. The sulfate, calcium, and magnesium values underwent evident decreases during the flood events, due to the arrival of less mineralized neo-infiltration water. Very small variations were observed for bicarbonates. The S10\_4 sample in Figure 5a (dotted line) represents an intermediate phase between flood and lean periods. In the Fuse spring (Figure 5b, Supplementary Tables S1 and S2), the lean period was characterized by bicarbonate–calcic–magnesian facies, while, during the flood period, bicarbonate–calcic facies were observed. Even in this case, the most evident variations concerned the magnesium and the sulfate values, with showy decreases during the flood period. For both springs, the alkali and chloride ion variations observed were not very important, due to the very low concentration of these ions.

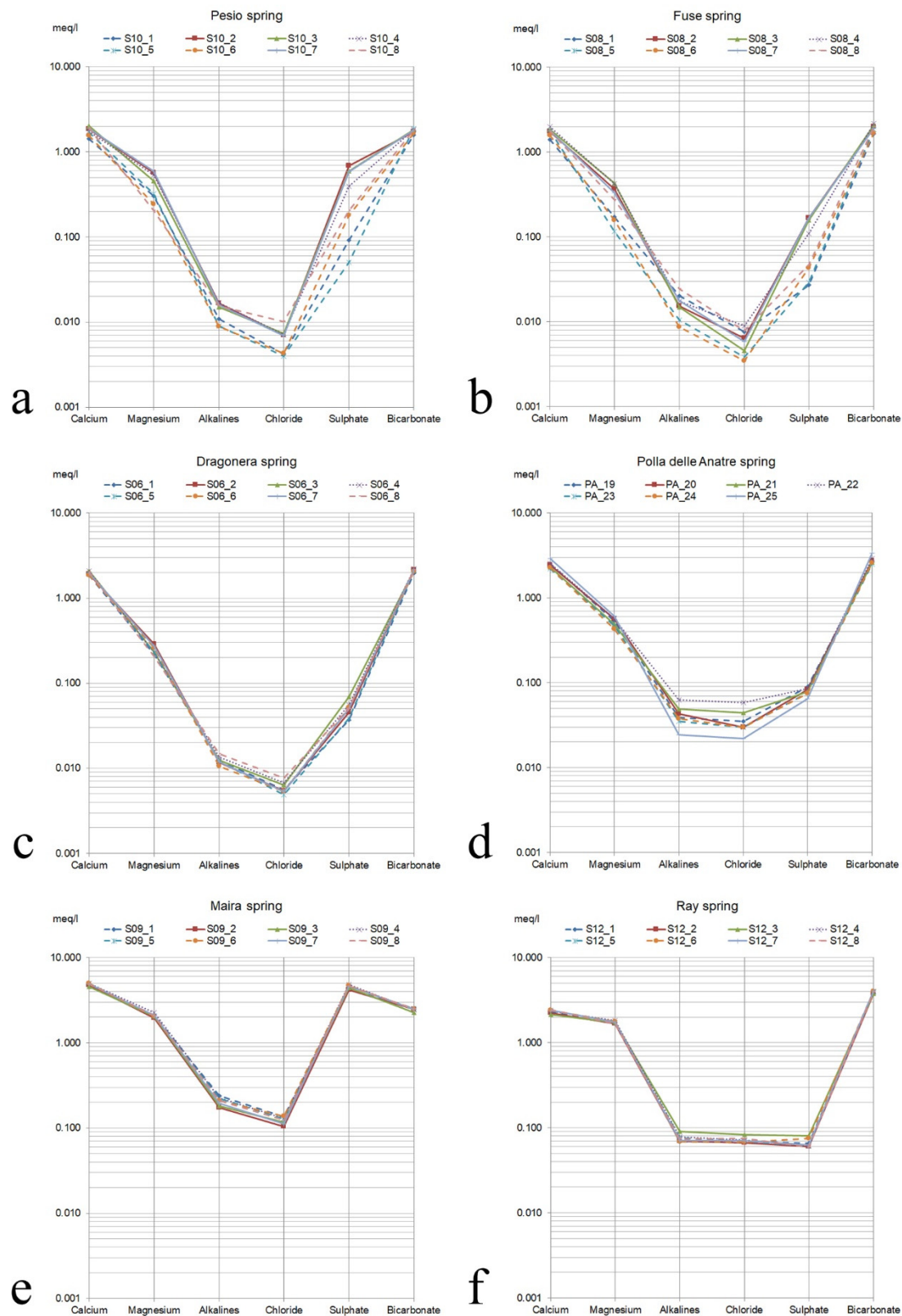


**Figure 5.** Schoeller diagram of the six examined springs. Lean periods are evidenced by continuous lines; flood periods are evidenced by dotted lines. (a) Pesio spring, system with dominant drainage; (b) Fuse spring, system with dominant drainage; (c) Dragonera spring, system with interconnected drainage; (d) Polla delle anatre spring, system with interconnected drainage; (e) Maira spring, system with dispersive circulation; (f) Ray spring, system with dispersive circulation.

### 3.2. Systems with Interconnected Drainage and Piston Flow Phenomenon

The Dragonera and Polla delle anatre springs are fed by relatively karstified aquifers. The hydrodynamic regime of these springs is rather variable, conditioned by infiltrative processes. During flooding events, the neo-infiltration water provides a significant increase in water levels (pressure waves), remobilizing the circulating water in the fractured areas of the rock massif and increasing the chemical–physical parameters of water such as T and EC (piston flow phenomenon). This subterranean water is characterized by rather low velocity flows. Data represented in Figure 3c,d show a year of monitoring Dragonera and Polla delle anatre spring parameters, respectively, from February 2014 to January 2015 and from December 2017 to November 2018.

In the winter period, the flow rates show reduced and constant values over time conditioned by low air temperatures and snowfall. The Dragonera spring Q was around 90 L/s, while the water EC and T values were about 230  $\mu\text{S}/\text{cm}$  and 7.05  $^{\circ}\text{C}$ , respectively (Figure 3c). Around the middle of March, the first slight increase in Q occurred, reaching 500 L/s, conditioned by snow melt processes. The water EC and T values rose to 250  $\mu\text{S}/\text{cm}$  and 7.40  $^{\circ}\text{C}$ , due to piston flow phenomenon. During the spring season, the Q was also influenced by the contribution of rain events, reaching even 1950 L/s. Furthermore, the water EC and T values slightly decreased, reaching values of 210  $\mu\text{S}/\text{cm}$  and 6.5  $^{\circ}\text{C}$ . Toward the middle of June, due to heavy rains, the flow rate had a peak, reaching 2586 L/s, with a water EC increase up to 225  $\mu\text{S}/\text{cm}$  and 6.90  $^{\circ}\text{C}$  (piston flow phenomenon). In the summer season, the flow rate decreased progressively, reaching a value of 78 L/s at the beginning of November. Water EC and T values did not show substantial changes. With the abundant autumn rainfall, Q reached 2212 L/s with a series of positive EC and T peaks, linked to the water residing in the system remobilization. The EC values reached 260  $\mu\text{S}/\text{cm}$ , while T rose to 7.40  $^{\circ}\text{C}$ . For the event of 4 November 2014 (Figure 4c), a marked piston flow phenomenon was shown.

Polla delle anatre (Figure 3d) is characterized by an evident piston flow phenomenon. The flow rate remained constant throughout the year, even after long periods of absence of contributions. Only during important infiltrative events did rapid and temporary water flow increase occur, accompanied by positive water EC and T peaks. In winter, the flow rate was around 0.5 L/s, the EC was about 260  $\mu\text{S}/\text{cm}$ , and T reached 9.95  $^{\circ}\text{C}$ , except for an anomalous event related to the rains occurring in the first week of January, which caused a temporary increase of the values (Q: 2.5 L/s, EC: 326  $\mu\text{S}/\text{cm}$ , T: 10.40  $^{\circ}\text{C}$ ). In spring, as a result of the water infiltration due to the snow melt, characterized by a T of about 0  $^{\circ}\text{C}$ , the flow rate showed a progressive increase, reaching 1.6 L/s. EC and T rose to 320  $\mu\text{S}/\text{cm}$  and 10.30  $^{\circ}\text{C}$ , respectively. This flood lasted until the end of April when the snow cover melted completely. Soft fluctuations in the water flow values, conditioned by air temperatures and solar radiation, were present. At the beginning of May, as a result of the abundant rainfall, the flow rate increased quickly, reaching 2.6 L/s in only 14 h, accompanied by an increase in water EC and T values to 40  $\mu\text{S}/\text{cm}$  and 0.3  $^{\circ}\text{C}$ , respectively. In about 15 days, the hydrodynamic and chemical–physical parameters of water returned to the lean values. Until June, there were still two episodes of flood with the same aquifer response. The whole summer period was characterized by a remarkable stability of Q (0.5 L/s), EC (260  $\mu\text{S}/\text{cm}$ ), and T (9.95  $^{\circ}\text{C}$ ) values. With the important October and November precipitations, a series of flood peaks occurred. Very fast increments and decreases in Q, EC, and T values with a duration of 2–3 days occurred. In the 8 January 2018 event (Figure 4d), Q rose from 0.49 to 2.6 L/s in about 1 day. Gradually, the water flow decreased, reaching the lean value after 8 days. The water EC rose from 260 to 325  $\mu\text{S}/\text{cm}$ , following a slow decrease, while the water T increased quickly from 9.95 to 10.46  $^{\circ}\text{C}$ , before progressively dropping to the pre-event values within 10 days.

In the Dragonera and Polla delle anatre springs, the striking differences evident in the previous cases were not visible, mainly because the springs did not reach quickly the neo-infiltration water, due to the presence of a large saturated area tending to homogenize the external signal (Supplementary Tables S1 and S2). The continuous acquisition of the EC

values permits following every change over time in detail, while the spot water sampling hinders grasping the flood peak during more evident piston flow phenomenon. In fact, samples were taken few days after the peak, and the values of the main ions did not differ significantly from those of the lean period. In the Dragonera spring (Figure 5c), samples S06\_1, S06\_5 and S06\_6 were taken at the end of the flood peak and had calcium, magnesium, sulfate, and bicarbonate concentrations very similar to the lean period samples. Its facies were bicarbonate–calcium (Figure 5c). In the Polla delle anatre spring, the facies were slightly bicarbonate–calcic–magnesian (Figure 5d, Supplementary Tables S1 and S2). Sample PA\_25 was taken at a flood peak; therefore, a weak increase in calcium and bicarbonate content, highlighting a more mineralized water arrival, was observed (Figure 5d). These waters were more mineralized because they were resident in the aquifer for longer periods and, therefore, had greater water–rock contact.

### 3.3. Systems with Dispersive Circulation and Chemical Signal Homogenization Phenomenon

The Maira and Ray springs are fed by aquifers characterized by the presence of predominantly dolomitic carbonate rocks, featuring by a very significant fracturing and a very reduced deep karstification. The deep groundwater circulation is driven mainly by the geometry of the impermeable rocks of the metamorphic basement toward the spring zone. Therefore, the underground flow velocity is reduced with a remarkable contact between water and rock. Consequently, the spring water is characterized by very high values of mineralization, and the water EC and T values are constant over time. Data presented in Figure 3e,f show 1 year of monitoring Maira and Ray spring parameters, respectively, from November 2013 to October 2014 and from January 2013 to December 2014.

Maira spring is characterized by Q fluctuations, due to the imperfect calm tank building where the water level measurement was carried out. The spring is fed by a high mountain karst aquifer related to very significant contributions from snow melt processes and abundant autumn rainfall. In winter, the Q showed a slight decrease from 900 L/s (November) to 630 L/s (April). The water EC and T values remained constant (about 680  $\mu\text{S}/\text{cm}$  and 6.50  $^{\circ}\text{C}$ ). In April, there was a slight but constant increase in Q, linked to the snow melting processes and to the spring rainfall until June, reaching the maximum annual value (1200 L/s). The flow rate then showed a modest decrease until the end of October (1050 L/s). The water EC was affected by the water flow variations and had a series of oscillations (10–20  $\mu\text{S}/\text{cm}$ ), reaching the minimum value of 650  $\mu\text{S}/\text{cm}$  in July. A progressive increase in EC values was observed until the end of October (690  $\mu\text{S}/\text{cm}$ ). In springtime, the water T was slightly marked, even if the Q increased due to the snow melt processes, decreasing by only 0.1  $^{\circ}\text{C}$ . The minimum annual T value was reached in the middle of June (6.44  $^{\circ}\text{C}$ ). The water T values rose until mid-September, again reaching 6.50  $^{\circ}\text{C}$ , before decreasing to 6.40  $^{\circ}\text{C}$  at the end of October. Therefore, the trend of water chemical and physical parameters was related to the homogenization phenomenon, conditioned by a very slow water circulation, dispersed in the network of the rock fractures.

The Ray spring is fed by a carbonate aquifer of small dimensions. The flow rate from January to March went from 17 to 16 L/s, and then rose gradually reaching the maximum annual value of 30 L/s at the beginning of June. In summer, the Q decreased regularly until mid-November, recording a value of 18 L/s. Following the abundant autumn rainfall, the Q showed a modest increase of only 2 L/s, stabilizing finally around 20 L/s in December. The EC value remained extremely constant throughout the year, varying from 378 to 350  $\mu\text{S}/\text{cm}$ . The water T showed only a slight increase in the summer season, from a minimum of 10.16  $^{\circ}\text{C}$  to a maximum of 10.36  $^{\circ}\text{C}$ , probably conditioned by the heating of the water intake station.

In these systems, the homogenization phenomenon is evidenced by the absolute constancy of all ions and, therefore, of the hydrogeochemical facies of the water sampled under different flow conditions (Figure 5e,f, Supplementary Tables S1 and S2). In the Maira spring, the facies was always sulfate–calcium with a bicarbonate–magnesian sub-facies (Figure 5e). This was probably due to the presence of gypsum and Carniola at the base of



the carbonate sequence. A constant bicarbonate–calcic–magnesian facies was observed in the Ray spring (Figure 5f), with a very low concentration of sulfates, typical of dolomitic rocks. The remarkable constancy of all ions found in the sample analysis, taken under different conditions, shows how these springs belong to systems characterized by the homogenization of the geochemical data, due to the slow circulation of water in very fractured rocks without major karst pipes.

#### 4. Conclusions

The hydrodynamic and the chemical–physical parameters of water can be influenced by the fracturing and/or karstification of the rock mass, its lithological characteristics, the geometry of the entire drainage network, and the phreatic zone size and thickness. High-frequency monitoring data of groundwater flow, electric conductivity, and temperature allow understanding the functioning of an aquifer and characterizing the system's response to the major infiltration events. On the basis of the monitoring data, three different kinds of aquifers in carbonate rock can be outlined (systems with dominant drainage, systems with interconnected drainage, and systems with dispersive circulation). In the dominant drainage systems, a rapid decrease in water electric conductivity and temperature is observed during the main floods, as exhibited by monitoring data of Pesio and Fuse springs (prevalent substitution phenomenon). In the interconnected drainage systems, an increase in water electric conductivity and temperature is observed during significant flow rate increase, as evidenced by monitoring data of Dragonera and Polla delle anatre (piston flow phenomenon). Lastly, the dispersive circulation systems show constant water electric conductivity and temperature values, linked to the slow circulation in the rock cluster, as highlighted by monitoring data of Maira and Ray (homogenization phenomenon).

The water sampling and chemical analysis of the main ions carried out during different hydrodynamic conditions, especially during lean and flood periods, reinforce the monitoring data. Chemical analyses highlight the parameters that cause electric conductivity variations in the lean and full periods in systems with dominant or interconnected drainage, as well as the absolute uniformity of the chemical data in the systems with dispersive circulation. Mineralization variations are clear in systems with dominant drainage, while they are less evident in systems with interconnected drainage. Various intermediate situations exist, and the drainage network organization can differ, both vertically and horizontally. However, on the basis of spring hydrography and hydro-chemical monitoring, it is always possible to refer to one of these models for describing a karst system. This work underlines the importance of high-frequency monitoring of water flow rate, electric conductivity, and temperature to distinguish the different types of aquifers set in carbonate rocks.

**Supplementary Materials:** The following are available online at <https://www.mdpi.com/article/10.3390/w14030441/s1>: Table S1. Values of the chemical–physical parameters and of the content of the main ions (TH = Total hardness expressed in French degrees); Table S2. Content of the main ions expressed in meq/L, values of the characteristic ratios and saturation index (SI) relating to dolomite and Cal.

**Author Contributions:** Conceptualization, V.B., A.F., and B.V.; methodology, A.F. and B.V.; validation, V.B., A.F., and B.V.; formal analysis, V.B., A.F., and B.V.; investigation, A.F. and B.V.; resources, A.F. and B.V.; data curation, V.B. and A.F.; writing—original draft preparation, V.B., A.F., and B.V.; writing—review and editing, V.B., A.F., and B.V.; visualization, V.B. and A.F.; supervision, B.V.; funding acquisition, A.F. and B.V. All authors read and agreed to the published version of the manuscript.

**Funding:** This research was funded by Regione Piemonte, Assessorato Ambiente, Energia, Innovazione e Ricerca (MORIS Project) and ALCOTRA 2007–2013—ALIRHYS Project (Alpi Latine—Identificazione delle risorse Hydrique Sotterranee).

**Acknowledgments:** The authors are grateful to the three anonymous reviewers for useful comments and suggestions, and to Marina Colonna and Camila Mori De Oliveira for the English revision of the manuscript.

**Conflicts of Interest:** The authors declare no conflict of interest.

## References

- Benischke, R.; Zojer, H.; Fritz, P.; Maloszewski, P.; Stichler, W. Environmental and artificial tracer studies in an Alpine karst massif (Austria). In Proceedings of the Karst Hydrogeology and Karst Environment Protection, Guilin, China, 10–15 October 1988; pp. 938–947.
- Braun, L.N. *Simulation of Snowmelt-Runoff in Lowland and Lower Alpine Regions of Switzerland*; ETH Zurich: Zurich, Switzerland, 1984.
- Hottelet, C.; Braun, L.; Leibundgut, C.; Rieg, A. Simulation of snowpack and discharge in an alpine karst basin. *Int. Assoc. Hydrol. Sci.* **1993**, *218*, 249–260.
- Moindrot, P.; Chauve, P.; Mania, J. Influence de L’enneigement sur L’hydrologie du Bassin Expérimental des Fourgs (Franche-Comté, France). In Proceedings of the Quatrième Colloque D’Hydrologie en Pays Calcaire et en Milieu Fissuré, Besançon, France, 29 September–1 October 1988; pp. 121–129.
- Chauve, P.; Mania, J.; Moindrot, D. Modalités de la fonte de neige en moyenne montagne et alimentation du karst sous-jacent. In *Hydrology in Mountainous Regions. I Hydrological Measurements*; IAHS Press: Wallingford, UK, 1990.
- Maire, R. Les montagnes-refuges calcaires de Méditerranée orientale et du Moyen-Orient (Grèce, Crète, Turquie, Iran). *Karstologia* **1990**, *15*, 13–24. [\[CrossRef\]](#)
- Borsato, A. Characterisation of a high-altitude alpine karst aquifer by means of temperature, conductivity and discharge monitoring (Centonia spring, Brenta Dolomites, N-Italy). In Proceedings of the 7th Conference on Limestone Hydrology and Fissured Media, Besançon, France, 20–22 September 2001; pp. 51–54.
- Nanni, T.; Rusi, S. Idrogeologia del massiccio carbonatico della montagna della Majella (Appennino centrale). *Boll.-Soc. Geol. Ital.* **2003**, *122*, 173–202.
- Fiorillo, F.; Guadagno, F.M. Long karst spring discharge time series and droughts occurrence in Southern Italy. *Environ. Earth Sci.* **2012**, *65*, 2273–2283. [\[CrossRef\]](#)
- Einsiedl, F.; Maloszewski, P.; Stichler, W. Multiple isotope approach to the determination of the natural attenuation potential of a high-alpine karst system. *J. Hydrol.* **2009**, *365*, 113–121. [\[CrossRef\]](#)
- Goldscheider, N.; Hötzl, H. Hydrogeological characteristics of folded alpine karst systems exemplified by the Gotesacker Plateau (German-Austrian Alps). *Acta Carsologica* **1999**, *28*, 87–103.
- Gremaud, V.; Goldscheider, N.; Savoy, L.; Favre, G.; Masson, H. Geological structure, recharge processes and underground drainage of a glacierised karst aquifer system, Tsanfleuron-Sanetsch, Swiss Alps. *Hydrogeol. J.* **2009**, *17*, 1833–1848. [\[CrossRef\]](#)
- Plan, L.; Decker, K.; Faber, R.; Wagreich, M.; Grasemann, B. Karst morphology and groundwater vulnerability of high alpine karst plateaus. *Environ. Geol.* **2009**, *58*, 285–297. [\[CrossRef\]](#)
- Vigna, B.; Banzato, C. The hydrogeology of high-mountain carbonate areas: An example of some Alpine systems in southern Piedmont (Italy). *Environ. Earth Sci.* **2015**, *74*, 267–280. [\[CrossRef\]](#)
- Torresan, F.; Fabbri, P.; Piccinini, L.; Dalla Libera, N.; Pola, M.; Zampieri, D. Defining the hydrogeological behavior of karst springs through an integrated analysis: A case study in the Berici Mountains area (Vicenza, NE Italy). *Hydrogeol. J.* **2020**, *28*, 1229–1247. [\[CrossRef\]](#)
- Maloszewski, P.; Stichler, W.; Zuber, A.; Rank, D. Identifying the flow systems in a karstic-fissured-porous aquifer, the Schneealpe, Austria, by modelling of environmental  $^{18}\text{O}$  and  $^3\text{H}$  isotopes. *J. Hydrol.* **2002**, *256*, 48–59. [\[CrossRef\]](#)
- Spadoni, M.; Brilli, M.; Giustini, F.; Petitta, M. Using GIS for modelling the impact of current climate trend on the recharge area of the S. Susanna spring (central Apennines, Italy). *Hydrol. Process. Int. J.* **2010**, *24*, 50–64. [\[CrossRef\]](#)
- Cichocki, G.; Zojer, H. VURAAS: Vulnerability and risk assessment for Alpine aquifer system. In *Groundwater Vulnerability Assessment and Mapping: IAH Selected Papers*; Witkowski, A.J., Kowalezyk, A., Vrba, J., Eds.; Taylor & Francis: London, UK, 2007; pp. 191–197.
- Boni, C.; Baldoni, T.; Banzato, F.; Cascone, D.; Petitta, M. Hydrogeological study for identification, characterization and management of groundwater resources in the Sibillini Mountains National Park (Central Italy). *Ital. J. Eng. Geol. Environ.* **2010**, *2*, 21–39.
- Amoruso, A.; Crescentini, L.; Petitta, M.; Tallini, M. Parsimonious recharge/discharge modeling in carbonate fractured aquifers: The groundwater flow in the Gran Sasso aquifer (Central Italy). *J. Hydrol.* **2013**, *476*, 136–146. [\[CrossRef\]](#)
- Galleani, L.; Vigna, B.; Banzato, C.; Russo, S.L. Validation of a vulnerability estimator for spring protection areas: The VESPA index. *J. Hydrol.* **2011**, *396*, 233–245. [\[CrossRef\]](#)
- Finger, D.; Hugentobler, A.; Huss, M.; Voinesco, A.; Wernli, H.; Fischer, D.; Weber, E.; Jeannin, P.-Y.; Kauzlaric, M.; Wirz, A. Identification of glacial meltwater runoff in a karstic environment and its implication for present and future water availability. *Hydrol. Earth Syst. Sci.* **2013**, *17*, 3261–3277. [\[CrossRef\]](#)
- Labat, D.; Ababou, R.; Mangin, A. Wavelet analysis in karstic hydrology. 1st part: Univariate analysis of rainfall rates and karstic spring runoffs. *C. R. L’Acad. Sci. Ser. IIA Earth Planet. Sci.* **1999**, *329*, 873–879.
- Nistor, M.-M. Groundwater Vulnerability in the Piedmont Region under Climate Change. *Atmosphere* **2020**, *11*, 779. [\[CrossRef\]](#)
- Fleury, P.; Plagnes, V.; Bakalowicz, M. Modelling of the functioning of karst aquifers with a reservoir model: Application to Fontaine de Vaucluse (South of France). *J. Hydrol.* **2007**, *345*, 38–49. [\[CrossRef\]](#)

26. White, W.B. Conceptual models for carbonate aquifers. *Groundwater* **1969**, *7*, 15–21. [[CrossRef](#)]
27. Mangin, A. L'approche hydrogéologique des karsts. *Spéléochronos* **1998**, *9*, 3–26.
28. Bakalowicz, M. Géochimie des eaux karstiques. Une méthode d'étude de l'organisation des écoulements souterrains. In Proceedings of the Deuxième Colloque d'Hydrologie en Pays Calcaire, Besançon, France, 6–10 October 1976; pp. 49–58.
29. Bakalowicz, M. Etude du degré d'organisation des écoulements souterrains dans les aquifères carbonates par une méthode hydrogéochimique nouvelle. *C. R. L'Acad. Sci.* **1977**, *284*, 2463–2466.
30. Banzato, C.; De Waele, J.; Fiorucci, A.; Vigna, B. Study of springs and karst aquifers by monitoring and geochemical analysis. In Proceedings of the 9th H2 Karst Conference on Limestone Hydrogeology, Besançon, France, 1–4 September 2011; pp. 1–3.
31. Bögli, A. *Karst Hydrology and Physical Speleology*; Springer: Berlin/Heidelberg, Germany, 1980.
32. Monnin, M.; Bakalowicz, M. Natural tracing in karst aquifers. In *Land and Marine Hydrogeology*; Taniguchi, M., Wang, K., Gamo, T., Eds.; Elsevier: Amsterdam, The Netherlands, 2003; pp. 93–114.
33. Shuster, E.T.; White, W.B. Seasonal fluctuations in the chemistry of lime-stone springs: A possible means for characterizing carbonate aquifers. *J. Hydrol.* **1971**, *14*, 93–128. [[CrossRef](#)]
34. Vigna, B. Monitoraggio e valutazione della vulnerabilità all'inquinamento degli acquiferi carsici. In Proceedings of the Le Risorse Idriche Sotterranee Delle Alpi Apuane: Conoscenze Attuali e Prospettive di Utilizzo, Massa, Italy, 22 June 2002; pp. 23–35.
35. Civita, M.; Manzone, L.; Vigna, B. Idrogeologia degli acquiferi carbonatici di alta quota: Due sistemi a confronto. In Proceedings of the Alpine Caves: Alpine Karst Systems and Their Environmental Context Asiago, Asiago, Italy, 11–14 June 1992; pp. 177–188.
36. Civita, M.; Olivero, G.; Pavia, R.; Vigna, B. Hydrodynamic and chemical features of an high altitude karstic system in the Maritime Alps (Italy). In Proceedings of the Water Resources in Mountainous Regions, Memoires, Lausanne, Switzerland; 1990; pp. 444–451.
37. Ford, D.; Williams, P.D. *Karst Hydrogeology and Geomorphology*; John Wiley & Sons: Hoboken, NJ, USA, 2013.
38. Ford, D.C.; Williams, P.W. *Karst Geomorphology and Hydrology*; Unwin Hyman London: London, UK, 1989; Volume 601.
39. Vigna, B. Schematizzazione e funzionamento degli acquiferi in rocce carbonatiche. *L'acqua Nelle Aree Carsiche Ital. Mem. Dell'istituto Ital. Speleol.* **2007**, *19*, 21–26.
40. Chen, Z.; Auler, A.S.; Bakalowicz, M.; Drew, D.; Griger, F.; Hartmann, J.; Jiang, G.; Moosdorf, N.; Richts, A.; Stevanovic, Z. The World Karst Aquifer Mapping project: Concept, mapping procedure and map of Europe. *Hydrogeol. J.* **2017**, *25*, 771–785. [[CrossRef](#)]
41. Panno, S.V.; Kelly, W.R.; Scott, J.; Zheng, W.; McNeish, R.E.; Holm, N.; Hoellein, T.J.; Baranski, E.L. Microplastic contamination in karst groundwater systems. *Groundwater* **2019**, *57*, 189–196. [[CrossRef](#)]
42. Hartmann, A.; Goldscheider, N.; Wagener, T.; Lange, J.; Weiler, M. Karst water resources in a changing world: Review of hydrological modeling approaches. *Rev. Geophys.* **2014**, *52*, 218–242. [[CrossRef](#)]
43. Wu, P.; Tang, C.; Zhu, L.; Liu, C.; Cha, X.; Tao, X. Hydrogeochemical characteristics of surface water and groundwater in the karst basin, southwest China. *Hydrol. Process. Int. J.* **2009**, *23*, 2012–2022. [[CrossRef](#)]
44. Bakalowicz, M. Karst groundwater: A challenge for new resources. *Hydrogeol. J.* **2005**, *13*, 148–160. [[CrossRef](#)]
45. Dreybrodt, W. *Processes in Karst Systems: Physics, Chemistry, and Geology*; Springer Science & Business Media: Berlin/Heidelberg, Germany, 2012; Volume 4.
46. Gunn, J. *Encyclopedia of Caves and Karst Science*; Taylor & Francis: Abingdon, UK, 2004.
47. Maire, R. Les karst de haute montagne dans le monde. In Proceedings of the Carso di Alta Montagna, Imperia, Italy, 30 April–4 May 1983; pp. 285–302.
48. Maire, R.; Nicod, J.; Chardon, M.; Delannoy, J.-J.; Laurent, R.; Lepiller, M.; Nicoud, G. Aperçus sur l'hydrologie karstique des Alpes occidentales. Systèmes karstiques et régimes des sources. *Karstologia* **1984**, *3*, 18–23. [[CrossRef](#)]